Exact time dependence of the cumulants of a tracer position in a dense lattice gas

Alexis Poncet,[1] Aurélien Grabsch,[2] Olivier Bénichou,[2] and Pierre Illien[3]

[1]*Univ. Lyon, ENS de Lyon, Univ. Claude Bernard, CNRS, Laboratoire de Physique, 69342 Lyon, France*

[2]*Sorbonne Université, CNRS, Laboratoire de Physique Théorique de la Matière Condensée (LPTMC), 4 Place Jussieu, 75005 Paris, France*

[3]*Sorbonne Université, CNRS, Physicochimie des Electrolytes et Nanosystèmes Interfaciaux (PHENIX), 4 Place Jussieu, 75005 Paris, France*

(Received 18 February 2022; revised 22 April 2022; accepted 3 May 2022; published 24 May 2022)

We develop a general method to calculate the exact time dependence of the cumulants of the position of a tracer particle in a dense lattice gas of hardcore particles. More precisely, we calculate the cumulant-generating function associated with the position of a tagged particle at arbitrary time, and at leading order in the density of vacancies on the lattice. In particular, our approach gives access to the short-time dynamics of the cumulants of the tracer position, a regime in which few results are known. The generality of our approach is demonstrated by showing that it goes beyond the case of a symmetric 1D random walk and covers the important situations of (1) a biased tracer, (2) comblike structures, and (3) d-dimensional situations.

DOI: 10.1103/PhysRevE.105.054139

I. INTRODUCTION

Understanding and characterizing tracer diffusion in crowded environments is central in numerous biological and physical contexts. In living systems, the interplay between the diffusion of tracer particles (fuelled by thermal fluctuations, active processes, or chemical reactions) and complex environments (which generally hinder their motion) controls many biological processes [1]. Quantifying tracer diffusion can also be used as a mean to probe the mechanical and rheological properties of different systems, such as colloidal suspensions or complex fluids, through passive and active microrheology [2–4].

These examples, in which the statistical properties of tracer particles are controlled by the interactions with their environment, are the motivation for a whole field of theoretical research. Among the different routes that were employed to characterize the statistics of diffusing particles in crowded environments, lattice gases of hardcore particles that jump at *exponentially distributed times* (often referred to as exclusion processes) have been the subject of many studies and have become central models of statistical mechanics [5,6]. For instance, such models have been used to predict the universal long-time tails of the velocity autocorrelation functions that were measured in the continuum [7–10]. Importantly, these models were also employed to compute the diffusion coefficient of a tracer particle. In dimension 2 or greater, different mean-field-like approximations were designed to estimate the diffusion coefficient of the tracer as a function of the density of the bath [11–13]. In the case of 1D systems, one can mention recent achievements which resulted in the derivation of exact results concerning tracer properties, including the calculation of its large deviations [14–17] and of bath-tracers correlations [18,19].

However, these results, whether exact or approximate, are generally valid only in the long-time limit, because their derivation relies on hydrodynamic limits or large deviations approaches [14–19]. A notable exception is provided in the dense limit by the approach by Brummelhuis and Hilhorst [20,21], later extended to the case of a biased tracer [22–25]. However, we stress that this approach is intrinsically *discrete in time*. Even though the real continuous-time description of exclusion processes, where particles jump at exponential times as defined above, is retrieved in the long-time limit, this approach fails to predict the dynamics of the tracer at short and intermediate times. So far, the only available results at arbitrary time concern the first cumulants in the low-density regime with immobile bath particles [26,27], the high-density regime for a symmetric tracer in one dimension [18], or the 1D situation at arbitrary density, but under a formulation that does not allow the derivation of fully explicit results [28]. Finally, a general quantitative description of the dynamics of the tracer for arbitrary time is lacking.

In this article, we fill this gap and calculate the exact and complete time dependence of the cumulants of a tracer particle in a dense lattice gas. We develop a general methodology which covers the important cases of (1) a biased tracer, (2) comblike structures, and (3) d-dimensional situations. These results fully quantify the dynamics of tracer particles in exclusion processes, which are paradigmatic models of statistical mechanics.

II. MODEL AND OUTLINE OF THE CALCULATIONS

We consider a lattice populated by particles at a density ρ between 0 and 1, which are initially positioned uniformly at random on the lattice, with the restriction that there can be only one particle per site. We adopt the usual dynamics of exclusion processes, which evolve in continuous time, and we assume that each particle has an exponential clock of time constant $\tau = 1$. When the clock ticks, each particle chooses to jump on one of its z neighboring sites with probability $1/z$. If the arrival site is empty, the jump is done. Otherwise, if the arrival site is occupied, the jump is canceled. Note that, in one dimension, this process corresponds to the celebrated symmetric exclusion process (SEP) [5,6].

The tagged particle (TP) is initially at the origin $\boldsymbol{x}(0) = 0$, and we study its displacement with time $\boldsymbol{x}(t) = [x_1(t), \dots, x_d(t)]$. We define the cumulant-generating function (CGF) $\psi(\boldsymbol{k}, t) \equiv \ln\langle e^{i\boldsymbol{k}\cdot\boldsymbol{x}(t)}\rangle$. We will consider the cumulants of the position projected onto one direction of the lattice, say, direction 1 $[x_1(t) = \boldsymbol{x}(t)\cdot\boldsymbol{e}_1]$:

$$\kappa_n(t) = \frac{1}{i^n}\left(\frac{\partial^n\psi(\boldsymbol{k}, t)}{\partial {k_1}^n}\right)_{\boldsymbol{k}=\boldsymbol{0}}. \tag{1}$$

Our goal here is the determination of the cumulant-generating function $\psi(\boldsymbol{k}, t)$ and the cumulants $\kappa_n(t)$ in the high-density limit $\rho \to 1$ and for arbitrary time t. We will define their rescaled high-density limit as $\bar{\kappa}_n = \lim_{\rho\to 1}\kappa_n/(1-\rho)$, where $\rho_0 = 1 - \rho$ is the density of vacancies on the lattice.

III. FROM A SINGLE VACANCY TO THE DENSE REGIME

Relying on the derivation that was originally proposed in a discrete-time description [20,21], we start by considering a system of finite size N in which all the sites are occupied except M of them (Fig. 1). We call these empty sites *vacancies*, and their fraction is denoted by $\rho_0 = M/N = 1 - \rho$. Now, in the high-density limit ($\rho_0 = M/N \to 0$), we note that the vacancies perform independent random walks and interact independently with the TP. We neglect events of order $O(\rho_0^2)$ in which two vacancies interact with each other, compared to events of order $O(\rho_0)$ in which one vacancy interacts with the TP. This gives exact results at linear order in the density of vacancies ρ_0. We call $p_1(\boldsymbol{x}|\boldsymbol{y}, t)$ the probability that, in a system with a single vacancy initially at $\boldsymbol{y}$, the TP has reached site $\boldsymbol{x}$ at time t knowing that it started from the origin. In Fourier space, the probability to find the tracer at a given location given that the vacancies were initially at positions $\boldsymbol{y}_1, \dots, \boldsymbol{y}_M$ can be written as a product of single-vacancy propagators p_1 (Appendix A). Averaging over the initial positions of the vacancies and taking the thermodynamic limit of $M, N \to \infty$

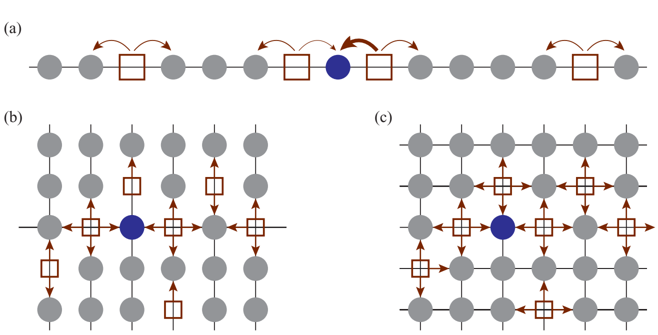

FIG. 1. For each of the considered geometries [1D (a), comb (b), 2D (c)], the continuous-time random walks of the particles are mirrored by the random walks of the vacancies (brown squares). The latter perform continuous-time nearest-neighbor symmetric random walks.

with fixed ρ_0, the cumulant-generating function reads

$$\lim_{\rho_0\to 0}\frac{\psi(\boldsymbol{k}, t)}{\rho_0} = \sum_{\boldsymbol{y}\neq 0}[\tilde{p}_1(\boldsymbol{k}|\boldsymbol{y}, t) - 1], \tag{2}$$

where we use the following convention for Fourier transforms: $\tilde{\phi}(\boldsymbol{k}) = \sum_{\boldsymbol{x}} e^{i\boldsymbol{k}\cdot\boldsymbol{x}}\phi(\boldsymbol{x})$. Let us emphasize the meaning of Eq. (2): the full probability law of a TP at high density is encoded in a much simpler quantity, namely, the propagator of the tracer in a system where there is only one vacancy. This expression is the continuous-time counterpart of the discrete-time approach [20,21].

Now, using standard techniques from the theory of random walks on lattices [29], we show how to express the single-vacancy propagator $p_1(\boldsymbol{x}|\boldsymbol{y}, t)$ in terms of first-passage time (FPT) densities associated with the random walks performed by the vacancies. We consider that there is only one vacancy on the lattice, initially at site $\boldsymbol{y}$. Let $f(\boldsymbol{0}|\boldsymbol{y}, t)$ be the probability that the vacancy arrives at the origin for the first time at t, and $f^*(\boldsymbol{0}|\boldsymbol{e}_\nu|\boldsymbol{y}, t)$ be the probability that the vacancy arrives at the origin for the first time at t, knowing that it was at site $\boldsymbol{e}_\nu$ right before reaching the origin. For simplicity, we will use the notation $\boldsymbol{e}_{-\mu} = -\boldsymbol{e}_\mu$ ($\mu \in \{\pm 1, \dots, \pm d\}$). The propagator $p_1(\boldsymbol{x}|\boldsymbol{y}, t)$ can be decomposed over the first passage of the vacancy on the origin:

$$\begin{aligned} p_1(\boldsymbol{x}|\boldsymbol{y}, t) &= \delta_{\boldsymbol{x},\boldsymbol{0}}\left(1 - \int_0^t d\tau\ f(\boldsymbol{0}|\boldsymbol{y}, t)\right) \\ &\quad + \sum_\nu \int_0^t d\tau\ p_1(\boldsymbol{x} - \boldsymbol{e}_\nu| - \boldsymbol{e}_\nu, t - \tau) f^*(\boldsymbol{0}|\boldsymbol{e}_\nu|\boldsymbol{y}, \tau), \end{aligned} \tag{3}$$

where the sum runs over all the directions $\nu \in \{\pm 1, \dots, \pm d\}$. One remarks that the same procedure can be applied to the total number n of arrivals of the vacancy at the origin before time t:

$$\begin{aligned} p_1(\boldsymbol{x}|\boldsymbol{y}, t) &= \delta_{\boldsymbol{y},\boldsymbol{0}}\left(1 - \int_0^t d\tau\ f(\boldsymbol{0}|\boldsymbol{y}, t)\right) \\ &\quad + \sum_{n=1}^\infty \int_0^\infty dt_1\cdots dt_n \int_0^t d\tau\ \delta\left(t - \sum_{i=1}^n t_i - \tau\right) \\ &\quad \times \sum_{\nu_1}\cdots\sum_{\nu_p}\delta_{\boldsymbol{e}_{\nu_1}+\dots+\boldsymbol{e}_{\nu_p},\boldsymbol{x}}\left(1 - \int_0^\tau d\tau'\ f(\boldsymbol{0}| - \boldsymbol{e}_{\nu_p}, t)\right) \\ &\quad \times f^*(\boldsymbol{0}|\boldsymbol{e}_{\nu_p}| - \boldsymbol{e}_{\nu_{p-1}}, t_n)\cdots f^*(\boldsymbol{0}|\boldsymbol{e}_{\nu_2}| - \boldsymbol{e}_{\nu_1}, t_2) \\ &\quad \times f^*(\boldsymbol{0}|\boldsymbol{e}_{\nu_1}|\boldsymbol{y}, t_2). \end{aligned} \tag{4}$$

These equations relate the single-vacancy propagator p_1 to the first-passage time densities f and f^*. Together with Eq. (2), these equations constitute the starting point of our analysis.

For clarity we consider separately: (1) the situation where the lattice is *treelike*, i.e., the situation where there is a single minimum-length path linking two arbitrary sites of the lattice (this will cover the case of one-dimensional and comb-like lattices) and (2) the situation where the lattice is *looped*, i.e., the situation where there is more than one minimum-length path linking two arbitrary sites of the lattice (this will cover the case of lattices of dimension 2 and higher).

IV. TREELIKE LATTICES

We first consider treelike lattices as shown in Figs. 1(a) and 1(b). We show in Appendix B that, on these geometries, the single-vacancy propagator (in Laplace domain) is simply related to the FPT densities through the relation

$$\hat{p}_1(k|\mathbf{y},u)=\frac{1}{u}\left[1+\left(e^{i\mu k}-1\right)\frac{1-\hat{f}_{-\mu}(u)}{1-\hat{f}_1(u)\hat{f}_{-1}(u)}\hat{f}(\mathbf{0}|\mathbf{y},u)\right], \tag{5}$$

where we introduce the shorthand notation $\hat{f}_\nu(u)=\hat{f}(\mathbf{0}|\boldsymbol{e}_\nu,u)$, and where we define the Laplace transform as $\hat{\varphi}(u)=\int_0^\infty dt\,\varphi(t)e^{-ut}$. One can use this expression in Eq. (2) to obtain the cumulant-generating function at high density in terms of first-passage quantities of a single vacancy. The last step consists in studying the random walk of a single vacancy to compute $\hat{f}(\mathbf{0}|\mathbf{y},u)$.

A. 1D lattice

We first apply this formalism to the case of a 1D lattice [Fig. 1(a)]. We consider the general situation of a biased tracer which jumps with probability p_+ to the right and p_- to the left ($s=p_+-p_-$ is the bias), initially at the origin, and in the presence of a single vacancy. We consider the random walk performed by the vacancy. It is surrounded by two particles with exponential clocks with ticking probability $\chi(t)=e^{-t}$ and its Laplace transform

$$\hat{\chi}(u)=\frac{1}{1+u}. \tag{6}$$

Except when it is next to the biased TP, the vacancy thus performs a symmetric Montroll-Weiss walk [29] with a distribution of jumping times given by $\chi(t)$. When the TP is not biased, the walk becomes symmetric for all sites. We first study this situation before accounting for defective sites next to the TP.

1. Unbiased TP

Let us call $f_y^{\rm UB}(t)$ the probability of first passage at the origin at time t of a vacancy initially at y, assuming that the TP is not biased ($p_{\pm1}=1/2, s=0$). The Montroll-Weiss walk (in continuous time) of the vacancy is linked to the associated discrete-time random walk by the formula [Ref. [29], Eq. (5.46)]

$$\hat{f}_y^{\rm UB}(u)=\hat{F}_y(\hat{\chi}(u)), \tag{7}$$

where $\hat{\chi}$ is given by Eq. (6), and $\hat{F}_y(\xi)=\sum_{t=0}^\infty \xi^t F_y(t)$ is the discrete Laplace transform of the probability of first passage at the origin of the discrete-time walk starting from y. It is known to be given [Ref. [29], Eq. (3.135)] by $\hat{F}_y(\xi)=\alpha^{|y|}$ with $\alpha=\xi^{-1}(1-\sqrt{1-\xi^2})$. We obtain the following expression for the first passage probability that we study:

$$\hat{f}_y^{\rm UB}(u)=\alpha^{|y|}, \tag{8}$$

$$\alpha=1+u-\sqrt{u(2+u)}. \tag{9}$$

One notes that α is a solution of the equation $\alpha^2-2(1+u)\alpha+1=0$, and this leads to the nontrivial relation

$$1+u=\frac{1+\alpha^2}{2\alpha}=\frac{1}{2}(\alpha+\alpha^{-1}). \tag{10}$$

Now that we have the expression for an unbiased TP, we turn to the case of a biased TP.

2. Biased TP

We consider a unique vacancy on the site $\nu=\pm1$, next to a biased TP. Two events can happen: either the TP jumps on site ν or the particle on site 2ν jumps on site ν. The first event is governed by an exponential law of rate (inverse time) p_ν, while the second is associated with an exponential clock of rate 1/2. The motion of the vacancy is thus governed by the exponential law of rate $(p_\nu+1/2)$, $\chi_V(t)=(p_\nu+1/2)e^{-(p_\nu+1/2)t}$. When such a jump of the vacancy occurs, there is a probability $p_\nu/(p_\nu+1/2)$ that it is done in the direction of the TP, and $(1/2)/(p_\nu+1/2)$ that it is done in the opposite direction.

We call $f_\nu(t)$ the probability of first passage of the vacancy at the origin, knowing that it starts from site ν. Either it is due to the first jump of the vacancy at time t, or the vacancy jumps on site 2ν at time $t_0<t$, comes back to site ν by a unbiased random walk at time t_0+t_1 and then arrives at the origin. This leads us to the relation

$$f_\nu(t)=p_\nu e^{-(p_\nu+1/2)t}+\int_0^t dt_0\frac{1}{2}e^{-(p_\nu+1/2)t_0}\times\int_0^{t-t_0}dt_1 f_1^{\rm UB}(t_1)f_\nu(t-t_0-t_1). \tag{11}$$

We compute the Laplace transform of this equation and remember that $\hat{f}_\nu^{\rm UB}(u)=\alpha$ with α given by Eq. (9). Moreover, $1+u$ and α are linked by Eq. (10). We end up with

$$\hat{f}_\nu(u)=\frac{p_\nu}{u+p_\nu+1/2-\alpha/2}=\frac{\alpha(1+\nu s)}{1+\nu s\alpha}, \tag{12}$$

where s is the bias. In particular, as expected, if $p_\nu=1/2$, $\hat{f}_\nu(u)=\hat{f}_\nu^{\rm UB}(u)=\alpha$.

Finally, considering a vacancy starting from site y and decomposing over the first visit to site $\mu=\mathrm{sgn}(y)$, we obtain

$$f_y(t)=\int_0^t dt_0 f_{|y|-1}^{\rm UB}(t_0)f_\mu(t-t_0), \tag{13}$$

and, in the Laplace domain,

$$\hat{f}_y(u)=\hat{f}_{|y|-1}^{\rm UB}(u)\hat{f}_\mu(u)=\frac{1+\mu s}{1+\mu s\alpha}\alpha^{|y|}. \tag{14}$$

Note that this scaling of the FPT with y ensures the convergence of the infinite sum involved in Eq. (2) Inserting the first-passage quantities computed in Eq. (14) into the expression of the propagator with a single vacancy [Eq. (5)], and then back into the expression of the cumulant-generating function [Eq. (2)], we obtain, after Laplace inversion:

$$\lim_{\rho_0\to0}\frac{\psi(k,t)}{\rho_0}=te^{-t}[I_0(t)+I_1(t)](\cos k-1+is\sin k), \tag{15}$$

where I_0 and I_1 are modified Bessel functions of the first kind [30]. In the unbiased case $s=0$, we retrieve previous

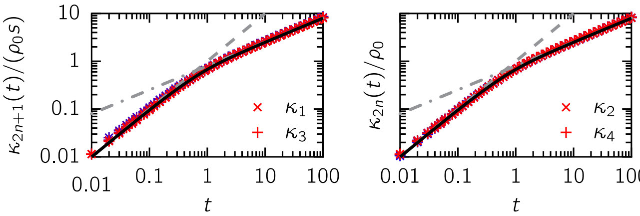

FIG. 2. Time dependence of the odd (left) and even (right) cumulants of a TP in 1D ($\rho_0 = 0.02$) for different values of the bias (from blue to red: $s = 0, 0.2, 0.5, 0.8, 1$). Symbols are the results from numerical simulations (see Appendix G for details). The black lines are the predictions from Eqs. (16) and (17); the gray lines are the asymptotic regimes at short and large times.

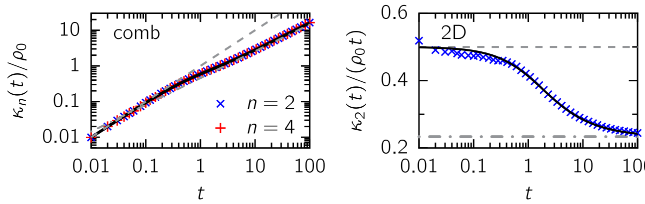

FIG. 3. Cumulants of the position of a tracer constrained to move on the backbone of a comb lattice (left) and on a 2D lattice, where we rescaled the data with time (right). Vacancy density $\rho_0 = 0.01$. The symbols correspond to the results from numerical simulations; the solid line is obtained from the inversion of the expression in Laplace domain [Eqs. (19) and (30)] using the Stehfest algorithm. The short-time (dashed line) and long-time (dash-dotted line) asymptotics are given in the text.

results for a symmetric tracer in the SEP [18]. The first implication is that we have the full time dependence of the even and odd cumulants,

$$\bar{\kappa}_{2n}(t) = te^{-t}[I_0(t) + I_1(t)], \tag{16}$$

$$\bar{\kappa}_{2n+1}(t) = ste^{-t}[I_0(t) + I_1(t)]. \tag{17}$$

At short time, we find that the cumulants obey $\bar{\kappa}_{2n}(t) \sim t$ and $\bar{\kappa}_{2n+1}(t) \sim st$. This means in particular that the fluctuations of the tracer are diffusive, and that the displacement of a biased TP κ_1 is ballistic. At large time, we retrieve the known expressions [14,23,31]: $\bar{\kappa}_{2n}(t) \sim \sqrt{2t/\pi}$ and $\bar{\kappa}_{2n+1}(t) \sim s\sqrt{2t/\pi}$. At all times, the results from Eqs. (16) and (17) are in perfect agreement with numerical simulations and shown in Fig. 2.

B. Comb lattice

We further illustrate the generality of our method by considering the important case of a comb lattice, a lattice made of a line, called the backbone, on which other lines, called the teeth, are connected [Fig. 1(b)]. This structure has been widely used to describe diffusion on percolation clusters [32]. From now on and for simplicity, we restrict ourselves to the case of a symmetric tracer constrained to move on the backbone of the lattice. Relying on the same methodology as before, the density of first-passage time to the origin of a vacancy starting from site (y_1, y_2) reads (Appendix C)

$$\hat{f}(0, 0|y_1, y_2; u) = \begin{cases} \hat{f}_1(\hat{f}_\parallel)^{|y_1|-1}\hat{f}_\perp \alpha^{|y_2|-1} & \text{if } y_2 \neq 0, \\ \hat{f}_1(\hat{f}_\parallel)^{|y_1|-1} & \text{if } y_2 = 0, \end{cases} \tag{18}$$

where we introduced the shorthand notations $\hat{f}_\mu = \hat{f}(0, 0|\mu, 0, u)$, $\hat{f}_\parallel = \hat{f}(1, 0|2, 0, u)$, and $\hat{f}_\perp = \hat{f}(1, 0|1, 1, u)$, which can all be easily expressed in terms of α. Using the results from Appendix C in Eq. (5), we finally obtain

$$\lim_{\rho_0 \to 0} \frac{\psi(k, u)}{\rho_0} = \hat{K}(u)(\cos k - 1),$$
$$\text{with } \hat{K}(u) = (2-\alpha)(\alpha^2 - \alpha + 2)/\{u(\alpha - 1) \times [u(2-\alpha) + \beta - 4\alpha + 6][u(\alpha - 2) + \beta + 2\alpha - 2]\}, \tag{19}$$

where $\beta = \sqrt{[(2+u)\alpha - 2u - 2][(3+u)\alpha - 2u - 4]}$. While odd cumulants are null [for symmetry reasons, and as can be seen from Eq. (19)], all the even cumulants are equal and given by $\hat{\kappa}_{\text{even}}(u) = \hat{K}(u)$. We deduce, after Laplace inversion, the short-time and long-time expansions: $K(t) \underset{t\to 0}{\sim} t$ and $K(t) \underset{t\to\infty}{\sim} \frac{2^{3/4}}{3\Gamma(3/4)} t^{3/4}$. Note that the long-time limit in the case of a symmetric tracer corresponds to the result we derived in discrete time [33]. For arbitrary time, we invert the cumulants numerically using the Stehfest algorithm. Numerical simulations are in perfect agreement with our analytical results (Fig. 3). Note that it is known that the two limits $t \to \infty$ and $\rho_0 \to 0$ do not commute, which mirrors the existence of a subtle ultimate diffusive regime [33], which we do not intend to describe here.

V. LOOPED LATTICES

We finally consider the key situation of d-dimensional lattices. Note that the geometry can be general, each of the spatial directions of the lattice being either infinite or finite with periodic boundary conditions, in such a way that the lattice remains translation-invariant. The CGF of the position of a symmetric tracer is derived following the same steps as previously: it is related to the single-vacancy propagators using Eq. (2), which are themselves related to the FPT densities of the vacancies through Eq. (4). However, by comparison with treelike lattices, the expression of the single-vacancy propagators in terms of the FPT densities is more complicated, because of the geometry of the system (details are given in Appendix D). The CGF now reads

$$\lim_{\rho_0 \to 0} \frac{\hat{\psi}(\boldsymbol{k}, u)}{\rho_0} = -\sum_{j=1}^{d} \hat{\Delta}(\boldsymbol{k}|\boldsymbol{e}_j, u)\hat{f}_j'(u), \tag{20}$$

where we defined $f_\nu'(t) = \sum_{\boldsymbol{y}\neq\boldsymbol{0}} f^*(\boldsymbol{0}|\boldsymbol{e}_\nu|\boldsymbol{y}; t)$ and

$$\hat{\Delta}(\boldsymbol{k}|\boldsymbol{e}_j, u) = \frac{2(1-\cos q_j)}{u} - \frac{1}{u}\sum_{\mu,\nu}\left(1 - e^{-i\boldsymbol{k}\cdot\boldsymbol{e}_\nu}\right) \times \{[\mathbf{I} - \mathbf{T}]^{-1}\}_{\nu,\mu} e^{i\boldsymbol{k}\cdot\boldsymbol{e}_\mu} \sum_{\epsilon=\pm 1} e^{-\epsilon i q_j} \hat{f}^*(\boldsymbol{0}|\boldsymbol{e}_\mu|\epsilon\boldsymbol{e}_j, u), \tag{21}$$

where $\mathbf{I}$ is the identity of size $2d$ and the matrix $\mathbf{T}$ has the entries $\mathbf{T}_{\mu,\nu} = e^{i\boldsymbol{k}\cdot\mathbf{e}_\nu}\hat{f}^*(\mathbf{0}|\boldsymbol{e}_\nu|-\boldsymbol{e}_\mu;u)$.

The final step of the calculation consists in determining the conditional FPT f^* in terms of well-known quantities, namely, the propagators associated with a discrete-time random walk on a lattice. The starting point of this calculation is the following relation, which consists in partitioning the random walk performed by the vacancy over the time of first visits to the origin:

$$\begin{aligned}\int_0^t dt_0 \frac{\chi(t_0)}{2d} p(\boldsymbol{e}_\mu|\boldsymbol{y}, t-t_0) &= \int_0^t dt_0 f^*(\mathbf{0}|\boldsymbol{e}_\mu|\boldsymbol{y}, t_0)\Psi(t-t_0)\\ &\quad + \int_0^t dt_0 \int_0^{t-t_0} dt_1 \, \frac{1}{2d}\chi(t-t_0-t_1) f(\mathbf{0}|\boldsymbol{y}, t_0) p(\boldsymbol{e}_\mu|\mathbf{0}, t_1),\end{aligned} \tag{22}$$

where $\Psi(t) = 1 - \int_0^t dt' \, \chi(t')$ is the probability that the walker did not move during a time t. It is then straightforward to express the conditional FPTs f^* in terms of the continuous-time occupation probabilities $p(\boldsymbol{r}|\boldsymbol{r}_0, t)$ (the probability to find a vacancy at site $\boldsymbol{r}$ at time t knowing that it started from site $\boldsymbol{r}_0$). Finally, relying on the relation between the propagators p and their discrete-time counterpart $P_{\boldsymbol{r}}^{(n)}$ (the probability to find the walker at site $\boldsymbol{r}$ after n steps knowing that it started from the origin) [29], we get the relations (Appendix E)

$$\hat{f}^*(\mathbf{0}|\boldsymbol{e}_\mu|\boldsymbol{y}, u) = \frac{\hat{\chi}}{2d}\left[\hat{P}_{\boldsymbol{e}_\mu-\boldsymbol{y}}(\hat{\chi}) - \frac{\hat{P}_{\boldsymbol{y}}(\hat{\chi})\hat{P}_{\boldsymbol{e}_\mu}(\hat{\chi})}{\hat{P}_{\mathbf{0}}(\hat{\chi}(u))}\right], \tag{23}$$

$$\hat{f}'_\mu(u) = \frac{1}{2d}\frac{\hat{\chi}}{1-\hat{\chi}}\left[1 - \frac{\hat{P}_{\boldsymbol{e}_\mu}(\hat{\chi})}{\hat{P}_{\mathbf{0}}(\hat{\chi})}\right], \tag{24}$$

where $\hat{P}_{\boldsymbol{r}}(\xi) = \sum_{n=0}^\infty P_{\boldsymbol{r}}^{(n)}\xi^n$ is the generating function associated with the discrete-time propagator $P_{\boldsymbol{r}}^{(n)}$.

In summary, the cumulant-generating function of the tracer position is fully determined in terms of the generating functions $\hat{P}$ associated with a discrete-time random walk on the considered lattice. Indeed, the expression of the CGF given in Eq. (20) simply involves f' and Δ. The former is related to the generating functions $\hat{P}$ through Eq. (24). The latter is related to the conditional first-passage densities $f^*(\mathbf{0}|\boldsymbol{e}_\mu|\boldsymbol{y}, t)$ through Eq. (21), which are themselves related to the generating functions $\hat{P}$ through Eq. (23). This result holds for any translation-invariant lattice, in arbitrary space dimension.

We now consider the example of the infinite 2D lattice. Making use of the symmetries of this lattice, one can show that the matrix $\mathbf{T}(\boldsymbol{k};u)$ takes the simple form

$$\mathbf{T}(\boldsymbol{k};u) = \begin{pmatrix} e^{ik_1}a(u) & e^{ik_1}a(u) & e^{ik_1}c(u) & e^{ik_1}c(u)\\ e^{-ik_1}a(u) & e^{-ik_1}a(u) & e^{-ik_1}c(u) & e^{-ik_1}c(u)\\ e^{ik_2}c(u) & e^{ik_2}c(u) & e^{ik_2}b(u) & e^{ik_2}a(u)\\ e^{-ik_2}c(u) & e^{-ik_2}c(u) & e^{-ik_2}a(u) & e^{-ik_2}b(u)\end{pmatrix}, \tag{25}$$

where we introduce shorthand notations for the following conditional FPT densities, which are determined in terms of the generating functions $\hat{P}$ using Eq. (23):

$$a(u) = f^*(\mathbf{0}|\boldsymbol{e}_1|\boldsymbol{e}_1, u) = \frac{\hat{\chi}(u)}{4}\left[\hat{P}(\mathbf{0}|\mathbf{0};\hat{\chi}(u)) - \frac{\hat{P}(\boldsymbol{e}_1|\mathbf{0};\hat{\chi}(u))^2}{\hat{P}(\mathbf{0}|\mathbf{0};\hat{\chi}(u))}\right], \tag{26}$$

$$b(u) = f^*(\mathbf{0}|\boldsymbol{e}_1|-\boldsymbol{e}_1, u) = \frac{\hat{\chi}(u)}{4}\left[\hat{P}(2\boldsymbol{e}_1|\mathbf{0};\hat{\chi}(u)) - \frac{\hat{P}(\boldsymbol{e}_1|\mathbf{0};\hat{\chi}(u))^2}{\hat{P}(\mathbf{0}|\mathbf{0};\hat{\chi}(u))}\right], \tag{27}$$

$$c(u) = f^*(\mathbf{0}|\boldsymbol{e}_1|\boldsymbol{e}_2, u) = \frac{\hat{\chi}(u)}{4}\left[\hat{P}(\boldsymbol{e}_1+\boldsymbol{e}_2|\mathbf{0};\hat{\chi}(u)) - \frac{\hat{P}(\boldsymbol{e}_1|\mathbf{0};\hat{\chi}(u))^2}{\hat{P}(\mathbf{0}|\mathbf{0};\hat{\chi}(u))}\right]. \tag{28}$$

Since we are interested only in the cumulants of the position projected onto one direction of the lattice, we consider only the dependence of the CGF on the component k_1 and set $k_2 = 0$ for simplicity. Using Eq. (20) yields the following expression of the CGF in terms of the conditional FPT densities:

$$\lim_{\rho_0\to 0}\frac{\hat{\psi}(k_1, k_2=0, u)}{\rho_0} = \frac{1}{2u}\frac{\hat{\chi}(u)}{1-\hat{\chi}(u)}\frac{(1-\cos k_1)(a-b-1)[(a+b-1)^2-4c^2]}{[2b(a+b-1)-4c^2]\cos k_1 + (a+b-1)(a^2-b^2-1) - 4(a-b)c^2}. \tag{29}$$

Finally, the CGF is expressed only in terms of four distinct propagators: $\hat{P}(\mathbf{0}|\mathbf{0};\xi)$, $\hat{P}(\boldsymbol{e}_1|\mathbf{0};\xi)$, $\hat{P}(2\boldsymbol{e}_1|\mathbf{0};\xi)$, and $\hat{P}(\boldsymbol{e}_1+\boldsymbol{e}_2|\mathbf{0};\xi)$. There exist relations between these propagators [20,21], as well as explicit expressions of them in terms of integrals, that eventually allow a fully explicit determination of the CGF.

As an example, we get the following expression of the second cumulant

$$\lim_{\rho_0\to 0}\frac{\hat{\kappa}_2(u)}{\rho_0} = \frac{1}{2u}\frac{\hat{\chi}(u)}{1-\hat{\chi}(u)}\frac{2-\hat{\chi}(u)g(\hat{\chi}(u))}{2+\hat{\chi}(u)g(\hat{\chi}(u))}, \tag{30}$$

where $g(\xi) = [\hat{P}_{\mathbf{0}}(\xi) - P_{2\boldsymbol{e}_1}(\xi)]/2$ and is given by the integral quantity [21,29]

$$g(\xi) = \frac{1}{(2\pi)^2}\int_{-\pi}^{\pi} dq_1 \int_{-\pi}^{\pi} dq_2 \, \frac{\sin^2 q_1}{1 - \frac{\xi}{2}(\cos q_1 + \cos q_2)}. \tag{31}$$

An explicit expression of $g(\xi)$ in terms of elliptic integrals, as well as its asymptotic expansions when $\xi \to 0$ and $\xi \to 1$, is given in Appendix F. This yields in particular the following asymptotics for the second cumulant in Laplace domain: $\hat{\kappa}_2(t) \underset{t\to 0}{\sim} t/2$ and $\hat{\kappa}_2(t) \underset{t\to\infty}{\sim} t/[2(\pi-1)]$. The expression given in Eq. (30) can be inverted back numerically into the time domain. The output of this inversion, together with numerical simulations and the short-time and long-time asymptotics, are represented in Fig. 3. The fluctuations of the tracer position go from one diffusive regime to another, and one observes that the long-time diffusion coefficient is approximately half the short-time diffusion coefficient.

VI. CONCLUSION

In this article we presented a methodology to compute the full and exact time dependence of the position of a tracer particle in a dense lattice gas. We demonstrated the generality of this method by considering different geometries (1D, comblike, d-dimensional) and obtaining fully explicit expressions (either in Laplace domain or in time domain) for the cumulants of the tracer position. These results unveil the transient time regimes that precede the long-time asymptotics, which are usually the only results that can be obtained from the standard approaches, such as hydrodynamic limits, large deviations, or discrete-time vacancy mediated diffusion. Although the method presented here holds in the dense limit, our results constitute a significant step in the description of the full time dynamics of tracer particles in exclusion processes.

APPENDIX A: FROM A SINGLE VACANCY TO THE DENSE REGIME

In this Appendix, we derive Eq. (2).

Let us consider a system of finite size N in which all the sites are occupied except M of them (Fig. 1). We call these empty sites *vacancies*, and their fraction is denoted by $\rho_0 = M/N = 1-\rho$. The high-density regime of the SEP corresponds to $\rho \to 1$. Instead of looking at the motion of the particles, one can equivalently study the motion of the vacancies. The later perform (*a priori* correlated) random walks on the lattice.

The tracer is initially at the origin, and its displacement at time t is $\boldsymbol{x}(t)$. This displacement can be said to be generated by the random walks of the vacancies: the tracer moves by exchanging its position with that of a neighboring vacancy. We number the vacancies and call $\boldsymbol{x}_j(t)$ the displacement of the TP generated by the jth vacancy. We have $\boldsymbol{x}(t) = \boldsymbol{x}_1(t) + \cdots + \boldsymbol{x}_M(t)$.

The initial positions of the vacancies are called $\boldsymbol{y}_j$. $P(\boldsymbol{x}|\boldsymbol{y}_1,\dots,\boldsymbol{y}_M,t)$ is the probability of a displacement $\boldsymbol{x}$ at time t knowing the initial positions of the vacancies. Similarly, $\mathcal{P}(\boldsymbol{x}_1,\dots,\boldsymbol{x}_M|\boldsymbol{y}_1,\dots,\boldsymbol{y}_M,t)$ is the probability that up to time t vacancies induced displacements $\{\boldsymbol{x}_j\}$ of the TP knowing their initial positions (see Fig. 1). By definition,

$$P(\boldsymbol{x}|\{\boldsymbol{y}_j\},t) = \sum_{\boldsymbol{y}_1,\dots,\boldsymbol{y}_M} \delta_{\boldsymbol{x},\boldsymbol{x}_1+\cdots+\boldsymbol{x}_M} \mathcal{P}(\boldsymbol{x}_1,\dots,\boldsymbol{x}_M|\boldsymbol{y}_1,\dots,\boldsymbol{y}_M,t). \quad \text{(A1)}$$

Now, in the high-density limit ($\rho_0 = M/N \to 0$), we assume that the vacancies perform independent random walks and interact independently with the TP. We neglect an event of order $O(\rho_0^2)$ in which two vacancies interact with each other, compared to events of order $O(\rho_0)$ in which one vacancy interacts with the TP. This gives exact results at linear order in the density of vacancies ρ_0. We call $p_1(\boldsymbol{x}|\boldsymbol{y},t)$ the probability that, in a system with a single vacancy initially at $\boldsymbol{y}$, the TP has displacement $\boldsymbol{x}$ at time t. Our assumption leads to

$$\mathcal{P}(\boldsymbol{x}_1,\dots,\boldsymbol{x}_M|\boldsymbol{y}_1,\dots,\boldsymbol{y}_M,t) \underset{\rho_0\to 0}{\sim} \prod_{j=1}^{M} p_1(\boldsymbol{x}_j|\boldsymbol{y}_j,t) \quad \text{(A2)}$$

with $\rho_0 = 1-\rho$. Equation (A1) now gives

$$P(\boldsymbol{x}|\boldsymbol{y}_1,\dots,\boldsymbol{y}_M,t) \underset{\rho_0\to 0}{\sim} \sum_{\boldsymbol{x}_1,\dots,\boldsymbol{x}_M} \delta_{\boldsymbol{x},\boldsymbol{x}_1+\cdots+\boldsymbol{x}_M} \times \prod_{j=1}^{M} p_1(\boldsymbol{x}_j|\boldsymbol{y}_j,t). \quad \text{(A3)}$$

We define the Fourier transform $\tilde{f}(\boldsymbol{k}) = \sum_{\boldsymbol{x}=-\infty}^{\infty} e^{i\boldsymbol{k}\cdot\boldsymbol{x}} f(\boldsymbol{x})$ and obtain

$$\tilde{P}(\boldsymbol{k}|\boldsymbol{y}_1,\dots,\boldsymbol{y}_M,t) \underset{\rho_0\to 0}{\sim} \prod_{j=1}^{M} \tilde{p}_1(\boldsymbol{k}|\boldsymbol{y}_j,t). \quad \text{(A4)}$$

We consider an initial condition in which the vacancies have equal probability to be on any site (except the origin). This corresponds to an equilibrated system and is known in the literature as *annealed* initial conditions. It can be opposed to the case of an initial frozen repartition of vacancies on the lattice, usually referred to as *quenched* initial conditions. Note that the choice of the type of initial conditions, annealed or quenched, can have a dramatic effect on the statistics of the position of the tracer, as studied recently in 1D geometries [16,34–36].

The cumulant-generating function of $\boldsymbol{x}(t)$ is the logarithm of the average of $\tilde{P}(\boldsymbol{k}|\boldsymbol{y}_1,\dots,\boldsymbol{y}_M,t)$,

$$\psi(\boldsymbol{k},t) = \ln \tilde{P}(\boldsymbol{k},t), \quad \text{(A5)}$$

where

$$\tilde{P}(\boldsymbol{k},t) \equiv \frac{1}{(N-1)^M} \sum_{\boldsymbol{y}_1,\dots,\boldsymbol{y}_M\neq 0} \tilde{P}(\boldsymbol{k}|\boldsymbol{y}_1,\dots,\boldsymbol{y}_M,t). \quad \text{(A6)}$$

In the limit $\rho_0 \to 0$, we obtain

$$\tilde{P}(\boldsymbol{k},t) \underset{\rho_0\to 0}{\sim} \left[\frac{1}{N-1}\sum_{\boldsymbol{y}\neq 0} \tilde{p}_1(\boldsymbol{k}|\boldsymbol{y},t)\right]^M \quad \text{(A7)}$$

$$= \left[1 + \frac{1}{N-1}\sum_{\boldsymbol{y}\neq 0} [\tilde{p}_1(\boldsymbol{k}|\boldsymbol{y},t) - 1]\right]^M. \quad \text{(A8)}$$

We consider the large-size limit $M, N \to \infty$ with $\rho_0 = M/N = 1-\rho$ constant. We obtain an expression for the propagator $\tilde{P}(\boldsymbol{k},t)$ in the high-density limit:

$$\tilde{P}(\boldsymbol{k},t) \sim \exp\left(\rho_0 \sum_{\boldsymbol{y}\neq 0} [\tilde{p}_1(\boldsymbol{k}|\boldsymbol{y},t) - 1)]\right), \quad \text{(A9)}$$

and for the cumulant-generating function:

$$\lim_{\rho_0\to 0} \frac{\psi(\boldsymbol{k},t)}{\rho_0} = \sum_{\boldsymbol{y}\neq 0} [\tilde{p}_1(\boldsymbol{k}|\boldsymbol{y},t) - 1], \quad \text{(A10)}$$

which coincides with Eq. (2).

APPENDIX B: SINGLE-VACANCY PROPAGATOR ON TREELIKE LATTICES

In this Appendix, we derive Eq. (5).

We consider the case of treelike lattices. In those specific geometries, when there is one vacancy on the lattice starting from site $\boldsymbol{y}$ [$\boldsymbol{y} = y_1$ in one dimension or $\boldsymbol{y} = (y_1, y_2)$ on a comb], the tracer can reach only two sites: $\mathbf{0}$ and $\pm \boldsymbol{e}_1$ (depending on whether the vacancy is initially at the right or at the left of the tracer). This implies $f^*(\mathbf{0}|\boldsymbol{e}_\mu|\boldsymbol{y},t) = f(\mathbf{0}|\boldsymbol{y},t)$ if $\boldsymbol{e}_\mu$ belongs to the shortest path from $\boldsymbol{y}$ to $\mathbf{0}$ and 0 otherwise. Equation (3) is then rewritten

$$p_1(x|\boldsymbol{y},t) = \delta_{\boldsymbol{y},\mathbf{0}}\left(1 - \int_0^t d\tau\ f(\mathbf{0}|\boldsymbol{y},t)\right) + \int_0^t d\tau\ p_1(x-\mu|-\boldsymbol{e}_\mu, t-\tau) f(\mathbf{0}|\boldsymbol{y},\tau), \tag{B1}$$

where $\mu \equiv \text{sgn}(y_1)$. Using the same simplification, Eq. (4) now reads

$$p_1(y|\boldsymbol{e}_\nu,t) = \sum_{n=0}^{\infty} \delta_{y,\nu[1-(-1)^{n+1}]} \times \int_0^\infty dt_1 \dots dt_n \int_0^\infty d\tau \delta\left(t - \sum_{i=1}^n t_i - \tau\right) \times [1 - f(\mathbf{0}|(-1)^n \boldsymbol{e}_\nu,\tau)] f(\mathbf{0}|(-1)^{n-1}\boldsymbol{e}_\nu,\tau) \times \cdots f(\mathbf{0}|-\boldsymbol{e}_\nu,t_2) f(\mathbf{0}|\boldsymbol{e}_\nu,t_1). \tag{B2}$$

We define the Fourier transform in space and Laplace transform in time by

$$\hat{\tilde{p}}_1(k|\boldsymbol{y},u) \equiv \sum_{Y=-\infty}^{\infty} e^{ikx} \int_0^\infty dt\ e^{-ut} p_1(x|\boldsymbol{y},t). \tag{B3}$$

Applying it to Eqs. (B1) and (B2), we obtain

$$\hat{\tilde{p}}_1(k|\boldsymbol{y},u) = \frac{1}{u} + \left[\hat{\tilde{p}}_1(k|-\boldsymbol{e}_\mu,u)e^{i\mu k} - \frac{1}{u}\right]\hat{f}(\mathbf{0}|\boldsymbol{y},u),$$
$$\hat{\tilde{p}}_1(k|\boldsymbol{e}_\nu,u) = \frac{1}{u}\frac{[1-\hat{f}_\nu(u)] + e^{i\nu k}\hat{f}_\nu(u)[1-\hat{f}_{-\nu}(u)]}{1-\hat{f}_1(u)\hat{f}_{-1}(u)}, \tag{B4}$$

where we introduce the shorthand notation $\hat{f}_\nu(u) = f(\mathbf{0}|\boldsymbol{e}_\nu,u)$. We combine the two equations and obtain the propagator of the displacement of the TP in term of the first passage probabilities of the vacancy,

$$\hat{\tilde{p}}_1(k|\boldsymbol{y},u) = \frac{1}{u}\left[1 + (e^{i\mu k}-1)\frac{1-\hat{f}_{-\mu}(u)}{1-\hat{f}_1(u)\hat{f}_{-1}(u)}\hat{f}(\mathbf{0}|\boldsymbol{y},u)\right], \tag{B5}$$

which corresponds to Eq. (5).

APPENDIX C: FPT ON A COMB

In this Appendix, we derive Eq. (19).

We consider the comb lattice represented in Fig. 1(b). The backbone of the lattice is the x_1 axis, and to each node of the backbone a 1D lattice is connected and extends infinitely in directions $\pm x_2$ (called teeth). Bath particles jump to each neighboring site with rate $1/4$ when they are on the backbone, and with rate $1/2$ when they are on the teeth. The tracer is constrained to move on the backbone and therefore jumps with rate $1/2$ to the right or to the left. Its position is denoted by $x(t)$, and the associated generating function is $\psi(k,t) = \ln\langle e^{ikx(t)}\rangle$.

Starting from Eq. (2), we write

$$\lim_{\rho\to 1}\frac{\psi(k,t)}{1-\rho} = \sum_{(y_1,y_2)\neq(0,0)} [\widetilde{p}_{y_1,y_2}(k,t) - 1], \tag{C1}$$

where the sum runs over all the sites different from the origin (all possible starting points of the vacancies). The quantity $p_{y_1,y_2}(x,t)$ is the probability that the tracer reaches site x at time t due to its interactions with a single vacancy that starts from site (y_1,y_2). Following the derivation in Appendix B, the Fourier-Laplace transform of the single-vacancy propagator is related to the FPT densities $\hat{f}$ through [Eq. (5)]

$$\begin{aligned}\hat{\widetilde{p}}_{y_1,y_2}(k,u) &= \frac{1}{u}\left[1 + (e^{i\mu k}-1)\frac{1-\hat{f}_{-\mu}(u)}{1-\hat{f}_1(u)\hat{f}_{-1}(u)}\hat{f}(0,0|y_1,y_2;u)\right] \\ &= \frac{1}{u}\left[1 + \frac{e^{i\mu k}-1}{1+\hat{f}_1(u)}\hat{f}(0,0|y_1,y_2;u)\right],\end{aligned} \tag{C2}$$

where $f(0,0|y_1,y_2,t)$ is the probability for a vacancy to reach the origin for the first time at time t starting from site (y_1,y_2). We also define $\hat{f}_\mu(u) = \hat{f}(0,0|\mu,0,u)$. We used the symmetry relation $\hat{f}_1 = \hat{f}_{-1}$ to obtain the second equality in Eq. (C2).

Because of the treelike structure of the lattice, there is a single path linking site (y_1,y_2) to the origin (0,0). This property ensures the relation [37]

$$f(0,0|y_1,y_2;t) = \int_0^t d\tau\ f(0,0|y_1',y_2',\tau) f(y_1',y_2'|y_1,y_2,t-\tau), \tag{C3}$$

or, in Laplace space,

$$\hat{f}(0,0|y_1,y_2;u) = \hat{f}(0,0|y_1',y_2',u)\hat{f}(y_1',y_2'|y_1,y_2,u). \tag{C4}$$

This relation holds for any site (y_1',y_2') belonging to the bath linking (y_1,y_2) and (0,0). Using the path decomposition $(y_1,y_2) \to (y_1,\text{sgn}(y_2)) \to (y_1,0) \to (\text{sgn}(y_1),0) \to (0,0)$, we write

$$\hat{f}(0,0|y_1,y_2;u) = \begin{cases} \hat{f}_1(u)\hat{f}_\parallel(u)^{|y_1|-1}\hat{f}_\perp(u)[\hat{f}(1,1|1,2,u)]^{|y_2|-1} & \text{if } y_2 \neq 0, \\ \hat{f}_1(u)\hat{f}_\parallel(u)^{|y_1|-1} & \text{if } y_2 = 0. \end{cases} \tag{C5}$$

For simplicity, we introduce the following notation:

$$\hat{f}(1,0|2,0,u) = \hat{f}_\parallel \tag{C6}$$

$$\hat{f}(1,0|1,1,u) = \hat{f}_\perp. \tag{C7}$$

We note that $\hat{f}(1,1|2,1,u)$, which denotes the FPT density between two neighboring sites of a tooth of the comb is nothing but the FPT density between two neighboring sites of a 1D lattice, and is given by

$$\hat{f}(1,1|2,1,u) = \alpha = 1 + u - \sqrt{u(2+u)}. \tag{C8}$$

Finally, using the expressions of the first-passage densities [Eq. (C5)], the single-vacancy propagator [Eq. (C2)], and the cumulant-generating function [Eq. (C1)] yields the following expression of the latter in Laplace domain:

$$\lim_{\rho\to 1}\frac{\psi(k,u)}{1-\rho}=\frac{1}{u}\frac{1}{1+\hat{f}_1(u)}\times\sum_{\epsilon=\pm 1}\sum_{y_2=-\infty}^{\infty}\sum_{y_1=1}^{\infty}(e^{i\epsilon k}-1)\hat{f}(0,0|\epsilon y_1,y_2;u) \tag{C9}$$

and eventually

$$\lim_{\rho\to 1}\frac{\psi(k,u)}{1-\rho}=\frac{1}{u}\frac{1}{1-\hat{f}_\parallel(u)}\times\left(1+\frac{2\hat{f}_\perp(u)}{1-\alpha(u)}\right)\frac{\hat{f}_1(u)}{1+\hat{f}_1(u)}2(\cos k-1). \tag{C10}$$

The last step of the calculation is to compute the quantities $\hat{f}_{\pm 1}$, $\hat{f}_\parallel$, and $\hat{f}_\perp$.

1. Calculation of $\hat{f}_1$

Here we follow the arguments that lead to the derivation of Eq. (11). Considering a vacancy initially located at site $(\pm 1,0)$ (on the backbone and right next to the tracer) and partitioning over the first jump performed by the vacancy, which can be directed either towards the tracer (with rate $1/2$) on the backbone and in the direction opposite to that of the tracer (with rate $1/4$) or sideways on the tooth of the comb (with rate $2\times 1/2$), one writes

$$\begin{aligned}f_1(t)=&\frac{1}{2}e^{-7t/4}\\&+\int_0^t dt_0\,\frac{1}{4}e^{-7t/4}\int_0^{t-t_0}dt_1\;f_\mu(t-t_0-t_1)f_\parallel^{\rm UB}(t_1)\\&+2\int_0^t dt_0\,\frac{1}{2}e^{-7t/4}\int_0^{t-t_0}dt_1\;f_\mu(t-t_0-t_1)f_\parallel^{\rm UB}(t_1),\end{aligned} \tag{C11}$$

where $f_\parallel$ is defined in Eq. (C6). Taking the Laplace transform of this equation, one gets

$$\hat{f}_1(u)=\frac{1/2}{u+\frac{7}{4}-\frac{1}{4}\hat{f}_\parallel-\hat{f}_\perp}. \tag{C12}$$

2. Calculation of $\hat{f}_\parallel$

In order to calculate $\hat{f}_\parallel=\hat{f}(1,0|2,0,u)$, we consider a vacancy starting from site (2,0) and, partitioning over the first jump performed by the vacancy which can be either on the backbone (with rate $2\times 1/4$) or sideways on the tooth of the comb (with rate $2\times 1/2$), we get

$$\begin{aligned}f_\parallel(t)=&\frac{1}{4}e^{-3t/2}\\&+\int_0^t dt_0\,\frac{1}{4}e^{-3t/2}\int_0^{t-t_0}dt_1\;f_\parallel(t-t_0-t_1)f_\parallel(t_1)\\&+2\int_0^t dt_0\,\frac{1}{2}e^{-3t/2}\int_0^{t-t_0}dt_1\;f_\parallel(t-t_0-t_1)f_\perp(t_1).\end{aligned} \tag{C13}$$

In Laplace space, one gets the equation satisfied by $\hat{f}_\parallel(u)$:

$$\hat{f}_\parallel(u)^2-4\left[u+\frac{3}{2}-\hat{f}_\perp(u)\right]\hat{f}_\parallel(u)+1=0. \tag{C14}$$

Choosing the solution satisfying the short-time condition $\lim_{u\to\infty}\hat{f}_\parallel(u)=0$, we get

$$\hat{f}_\parallel(u)=2\left(u+\frac{3}{2}-\hat{f}_\perp(u)\right)-\sqrt{4\left(u+\frac{3}{2}-\hat{f}_\perp(u)\right)^2-1}. \tag{C15}$$

3. Calculation of $\hat{f}_\perp$

Finally, in order to calculate $\hat{f}_\perp=\hat{f}(1,0|1,1,u)$, we consider a vacancy starting from site (1,1) and, partitioning over the first jump performed by the vacancy which can be either away from the backbone (with rate $1/2$) or towards the backbone (with rate $1/4$), we get

$$\begin{aligned}f_\perp(t)=&\frac{1}{4}e^{-3t/4}\\&+\int_0^t dt_0\,\frac{1}{2}e^{-3t/4}\int_0^{t-t_0}dt_1\;f_\perp(t-t_0-t_1)f_{\rm 1D}(t_1),\end{aligned} \tag{C16}$$

where $f_{\rm 1D}$ is the FPT density of a vacancy between two neighboring sites of a one-dimensional lattice [its Laplace transform is denoted by $\alpha(u)$ in the main text]. In Laplace space, we get

$$\hat{f}_\perp=\frac{1}{4u+3-2\alpha(u)}=\frac{\alpha}{2-\alpha}. \tag{C17}$$

Equation (C10), together with the expressions of $\hat{f}_\parallel$, $\hat{f}_\parallel$, and $\hat{f}_1$ above, leads after some algebra to Eq. (19).

APPENDIX D: LOOPED LATTICES: EXPRESSION OF THE CGF IN TERMS OF THE CONDITIONAL FPT f^*

In this Appendix, we derive Eq. (20).

We now turn to the case of d-dimensional lattices. We start from Eq. (A8), which relates the propagator of the tracer position to the single-vacancy propagators in Fourier space $\tilde{p}_1(\boldsymbol{k}|\boldsymbol{y},t)$:

$$\tilde{P}(\boldsymbol{k},t)\simeq\left[1+\frac{1}{N-1}\sum_{\boldsymbol{y}\neq 0}[\tilde{p}_1(\boldsymbol{k}|\boldsymbol{y},t)-1]\right]^M. \tag{D1}$$

Using the Fourier transform of Eq. (26), which relate the single-vacancy propagators of the random walk of a tracer starting from an arbitrary point $\boldsymbol{y}$ and from a site located at the vicinity of the tracer $\boldsymbol{e}_\nu$, we find the relation

$$\begin{aligned}\tilde{p}_1(\boldsymbol{k}|\boldsymbol{y},t)=&1-\int_0^t d\tau\;f(\boldsymbol{0}|\boldsymbol{y},t)\\&+\sum_\nu\int_0^t d\tau\;f^*(\boldsymbol{0}|\boldsymbol{e}_\nu|\boldsymbol{y};\tau)e^{iq_\nu}\tilde{p}_1(\boldsymbol{k}|-\boldsymbol{e}_\nu;t-\tau).\end{aligned} \tag{D2}$$

Replacing $\tilde{p}_1(\boldsymbol{k}|\boldsymbol{y},t)$ in Eq. (D1) by this expression, and using the relation $f(\boldsymbol{0}|\boldsymbol{y};t)=\sum_\nu f^*(\boldsymbol{0}|\boldsymbol{e}_\nu|\boldsymbol{y};t)$, one gets

$$\tilde{P}(\boldsymbol{k},t)=\left[1-\frac{1}{N-1}\sum_\nu\int_0^t d\tau\,[1-e^{iq_\nu}\tilde{p}_1(\boldsymbol{k}|\boldsymbol{e}_\nu;t-\tau)]\times\sum_{\boldsymbol{y}\neq\boldsymbol{0}}f^*(\boldsymbol{0}|\boldsymbol{e}_\nu|\boldsymbol{y};\tau)\right]^M. \tag{D3}$$

Using the equivalence between directions $\pm\boldsymbol{e}_\nu$, defining (for $j=1,\dots,d$)

$$\Delta(\boldsymbol{k}|\boldsymbol{e}_j,t)=2-e^{iq_j}\tilde{p}_1(\boldsymbol{k}|-\boldsymbol{e}_j;t)-e^{-iq_j}\tilde{p}_1(\boldsymbol{k}|\boldsymbol{e}_j;t), \tag{D4}$$

and taking the thermodynamics limit ($M,N\to\infty$ with fixed $\rho=M/N$), one gets

$$\tilde{P}(\boldsymbol{k},t)=\exp\left[-\rho\sum_{j=1}^d\int_0^t d\tau\,\Delta(\boldsymbol{k}|\boldsymbol{e}_j,t-\tau)f'_\nu(\tau)\right], \tag{D5}$$

where we defined

$$f'_\nu(t)=\sum_{\boldsymbol{y}\neq\boldsymbol{0}}f^*(\boldsymbol{0}|\boldsymbol{e}_\nu|\boldsymbol{y};t). \tag{D6}$$

In the Laplace domain, the CGF then reads

$$\lim_{\rho_0\to0}\frac{\hat{\psi}(\boldsymbol{k},u)}{\rho_0}=-\sum_{j=1}^d\hat{\Delta}(\boldsymbol{k}|\boldsymbol{e}_j,u)\hat{f}'_j(u). \tag{D7}$$

The last step of the calculation consists in expressing $\hat{\Delta}(\boldsymbol{k}|\boldsymbol{e}_j,u)$ in terms of the conditional FPT densities $f^*(\boldsymbol{0}|\boldsymbol{e}_\nu|\boldsymbol{e}_\mu,t)$. Taking the Fourier-Laplace transform of Eq. (4), we get

$$\hat{\tilde{p}}_1(\boldsymbol{k}|\boldsymbol{y};u)=\frac{1}{u}\left(1+\sum_\mu V_\mu(\boldsymbol{k};u)f^*(\boldsymbol{0}|\boldsymbol{e}_\mu|\boldsymbol{y};u)\right), \tag{D8}$$

where we defined

$$V_\mu(\boldsymbol{k};u)\equiv\sum_\nu[1-e^{-i\boldsymbol{k}\cdot\boldsymbol{e}_\nu}]\{[\mathbf{I}-\mathbf{T}(\boldsymbol{k};u)]^{-1}\}_{\nu,\mu}e^{i\boldsymbol{k}\cdot\boldsymbol{e}_\mu}. \tag{D9}$$

$\mathbf{I}$ is the identity of size $2d$, and the matrix $\mathbf{T}(\boldsymbol{k};u)$ has the entries $[\mathbf{T}(\boldsymbol{k};u)]_{\mu,\nu}$ defined by

$$\begin{aligned}[\mathbf{T}(\boldsymbol{k};u)]_{\nu,\mu}&=e^{i\boldsymbol{k}\cdot\boldsymbol{e}_\nu}\hat{f}^*(\boldsymbol{0}|\boldsymbol{e}_\nu|-\boldsymbol{e}_\mu;u)\\&=\int_0^\infty dt\ f_t^*(\boldsymbol{0}|\boldsymbol{e}_\nu|-\boldsymbol{e}_\mu,t)e^{-ut}.\end{aligned} \tag{D10}$$

Taking the Laplace transform of Eq. (D4) and using the expression of $\hat{\tilde{p}}_1$ [Eq. (D8)] yields

$$\hat{\Delta}(\boldsymbol{k}|\boldsymbol{e}_j,u)=\frac{2(1-\cos q_j)}{u}-\frac{1}{u}\sum_\mu V_\mu(\boldsymbol{k},u)\sum_{\epsilon=\pm1}e^{i\epsilon q_j}\hat{f}^*(\boldsymbol{0}|\boldsymbol{e}_\mu|-\epsilon\boldsymbol{e}_j,u). \tag{D11}$$

We then have an expression of the CGF in terms of the conditional first-passage densities f^* [Eq. (20)].

APPENDIX E: CONDITIONAL FPT DENSITIES f^* ON A LOOPED LATTICE

In this Appendix, we derive Eqs. (23) and (24).

Taking the Laplace transform of Eq. (22), using the renewal equation $\hat{f}(\boldsymbol{y}|\boldsymbol{0},u)=\hat{p}(\boldsymbol{y}|\boldsymbol{0},u)/\hat{p}(\boldsymbol{0}|\boldsymbol{0},u)$ (valid for $\boldsymbol{y}\neq\boldsymbol{0}$ [29]), and using $\hat{\Psi}(u)=(1-\hat{\chi}(u))/u$, we get

$$\hat{f}^*(\boldsymbol{0}|\boldsymbol{e}_\mu|\boldsymbol{y},u)=\frac{1}{2d}\frac{u\hat{\chi}(u)}{1-\hat{\chi}(u)}\left[\hat{p}(\boldsymbol{e}_\mu-\boldsymbol{y}|\boldsymbol{0},u)-\frac{\hat{p}(\boldsymbol{y}|\boldsymbol{0},u)\hat{p}(\boldsymbol{e}_\mu|\boldsymbol{0},u)}{\hat{p}(\boldsymbol{0}|\boldsymbol{0},u)}\right], \tag{E1}$$

where $p(\boldsymbol{r}|\boldsymbol{r}_0;t)$ is the propagator associated to a simple random walk on the considered lattice (the probability to find a walker at site $\boldsymbol{r}$ at time t knowing that it started from site $\boldsymbol{r}_0$ at time $t=0$), and we used the translational invariance of the lattice [i.e., $p(\boldsymbol{r}|\boldsymbol{r}_0;t)=p(\boldsymbol{r}-\boldsymbol{r}_0|\boldsymbol{0};t)$ for any two sites $\boldsymbol{r}$ and $\boldsymbol{r}_0$].

The Laplace transform of the continuous-time propagator can be related to the generating function $\hat{P}(\boldsymbol{r}|\boldsymbol{r}_0;\xi)=\sum_{n=0}^\infty P_n(\boldsymbol{r}|\boldsymbol{r}_0)\xi^n$ associated with the discrete-time propagator $P_n(\boldsymbol{r}|\boldsymbol{r}_0)$ (the probability to find the walker at site $\boldsymbol{r}$ after n steps knowing that it started from site $\boldsymbol{r}_0$) through the relation [29]

$$\hat{p}(\boldsymbol{r}|\boldsymbol{r}_0,u)=\frac{1-\hat{\chi}(u)}{u}\hat{P}(\boldsymbol{r}|\boldsymbol{r}_0;\hat{\chi}(u)), \tag{E2}$$

which yields

$$\hat{f}^*(\boldsymbol{0}|\boldsymbol{e}_\mu|\boldsymbol{y},u)=\frac{\hat{\chi}(u)}{2d}\left[\hat{P}(\boldsymbol{e}_\mu-\boldsymbol{y}|\boldsymbol{0};\hat{\chi}(u))-\frac{\hat{P}(\boldsymbol{y}|\boldsymbol{0};\hat{\chi}(u))\hat{P}(\boldsymbol{e}_\mu|\boldsymbol{0};\hat{\chi}(u))}{\hat{P}(\boldsymbol{0}|\boldsymbol{0};\hat{\chi}(u))}\right], \tag{E3}$$

which coincides with Eq. (23).

We finally compute $\hat{f}'_\mu(u)$, defined in Eq. (D6). To this end, we must use the normalization condition $\sum_{\boldsymbol{r}}P_n(\boldsymbol{r}|\boldsymbol{r}_0)=1$, which reads, in terms of the generating function associated with P_n,

$$\sum_{\boldsymbol{r}}\hat{P}(\boldsymbol{r}|\boldsymbol{r}_0,\xi)=\frac{1}{1-\xi}. \tag{E4}$$

With Eq. (23), we get the simple expression

$$\hat{f}'_\mu(u)=\frac{1}{2d}\frac{\hat{\chi}(u)}{1-\hat{\chi}(u)}\left[1-\frac{\hat{P}(\boldsymbol{e}_\mu|\boldsymbol{0},\hat{\chi}(u))}{\hat{P}(\boldsymbol{0}|\boldsymbol{0},\hat{\chi}(u))}\right], \tag{E5}$$

which is Eq. (24).

APPENDIX F: EXPLICIT EXPRESSION OF $g(\xi)$ IN TERMS OF ELLIPTIC INTEGRALS

The function g is defined in Eq. (31) as

$$g(\xi)\equiv\frac{1}{2}[\hat{P}(\boldsymbol{0}|\boldsymbol{0};\xi)-\hat{P}(2\boldsymbol{e}_1|\boldsymbol{0};\xi)] \tag{F1}$$

$$=\frac{1}{(2\pi)^2}\int_{-\pi}^{\pi}dq_1\int_{-\pi}^{\pi}dq_2\,\frac{\sin^2q_1}{1-\frac{\xi}{2}(\cos q_1+\cos q_2)}. \tag{F2}$$

can be expressed in terms of elliptic integrals:

$$g(\xi) = \frac{4}{\xi^2} + \frac{4}{\pi\xi^2\sqrt{1-\xi^2}}\left[(1-\xi)K\left(\frac{i\xi}{\sqrt{1-\xi^2}}\right) - (1-\xi^2)E\left(\frac{i\xi}{\sqrt{1-\xi^2}}\right) - 2\Pi\left(\frac{\xi}{\xi-1}, \frac{i\xi}{\sqrt{1-\xi^2}}\right)\right], \tag{F3}$$

where we use the following expressions for the elliptic integrals:

$$K(k) = \int_0^1 \frac{dt}{\sqrt{1-t^2}\sqrt{1-k^2t^2}}, \tag{F4}$$

$$E(k) = \int_0^1 dt \frac{\sqrt{1-k^2t^2}}{\sqrt{1-t^2}}, \tag{F5}$$

$$\Pi(\nu, k) = \int_0^1 \frac{dt}{(1-\nu t^2)\sqrt{1-t^2}\sqrt{1-k^2t^2}}. \tag{F6}$$

The asymptotic expansions of $g(\xi)$ read

$$g(\xi) \underset{\xi\to 1}{=} \left(2 - \tfrac{4}{\pi}\right) + \tfrac{2}{\pi}(1-\xi)\ln(1-\xi) + O(1-\xi), \tag{F7}$$

$$g(\xi) \underset{\xi\to 0}{=} \frac{1}{2} + \frac{3}{32}\xi^2 + O(\xi^3). \tag{F8}$$

APPENDIX G: NUMERICAL SIMULATIONS

The simulations of the SEP are performed on a periodic ring of size N, with $M = \rho N$ particles at average density ρ. In Fig. 2, $N = 2000$ and $M = 1960$ ($\rho_0 = 0.02$). The particles are initially placed uniformly at random. The jumps of the particles are implemented as follow. One first picks a particle uniformly at random. Then a direction (left or right) is chosen according to probabilities 1/2 and 1/2 for bath particles, and p_1 and $p_{-1} = 1 - p_1$ for the tracer. If the chosen particle has no neighbor in that direction, the jump is performed, otherwise it is rejected. In both cases, the time of the simulation is incremented by a random number picked from an exponential distribution of rate N. We keep track of the particle initially at the origin (the tracer) and compute the moments of its displacement, averaging over 2×10^6 simulations.

The simulations of the comb and of the 2D lattice (Fig. 3) are performed in a similar way. Starting from a uniform random configuration, particles are chosen uniformly at random and try to jump to neighboring sites with probabilities described in Fig. 4. Hard-core exclusion is enforced. In both cases (comb and 2D lattice), we use a periodic grid of size 100×100 with 9900 particles ($\rho_0 = 0.01$) and average over 4×10^6 simulations.

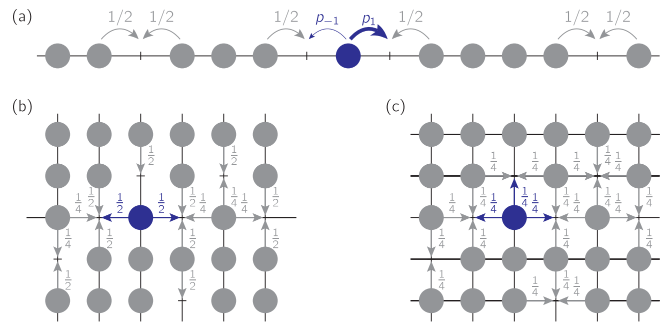

FIG. 4. (a) Symmetric exclusion process (SEP) with a biased TP. The bath particles jump on neighboring site with rate 1/2, whereas the jump rates of the TP are $p_{\pm 1} = (1 \pm s)/2$ where s is the bias. (b) Tracer diffusing on a crowded comb lattice. Particles jump on neighboring sites with rate 1/4 (resp. 1/2) when they are on the backbone (resp. the teeth) of the comb. The tracer is constrained to move on the backbone of the lattice. (c) Tracer diffusion on a crowded 2D lattice. The bath particles and the tracer jump on each neighboring site with rate 1/4.

[1] F. Höfling and T. Franosch, Rep. Prog. Phys. **76**, 046602 (2013).
[2] L. G. Wilson and W. C. K. Poon, Phys. Chem. Chem. Phys. **13**, 10617 (2011).
[3] T. M. Squires and T. G. Mason, Annu. Rev. Fluid Mech. **42**, 413 (2010).
[4] A. M. Puertas and T. Voigtmann, J. Phys.: Condens. Matter **26**, 243101 (2014).
[5] K. Mallick, J. Stat. Mech.: Theory Exp. (2011) P01024.
[6] T. Chou, K. Mallick, and R. K. P. Zia, Rep. Prog. Phys. **74**, 116601 (2011).
[7] T. M. Nieuwenhuizen, P. F. J. van Velthoven, and M. H. Ernst, Phys. Rev. Lett. **57**, 2477 (1986).
[8] P. J. H. Denteneer and M. H. Ernst, Phys. Rev. B **29**, 1755 (1984).
[9] T. M. Nieuwenhuizen and M. H. Ernst, J. Stat. Phys. **41**, 773 (1985).
[10] D. Frenkel, Phys. Lett. A **121**, 385 (1987).
[11] K. Nakazato and K. Kitahara, Prog. Theor. Phys. **64**, 2261 (1980).
[12] R. A. Tahir-Kheli and R. J. Elliott, Phys. Rev. B **27**, 844 (1983).
[13] H. van Beijeren and R. Kutner, Phys. Rev. Lett. **55**, 238 (1985).
[14] T. Imamura, K. Mallick, and T. Sasamoto, Phys. Rev. Lett. **118**, 160601 (2017).
[15] P. L. Krapivsky, K. Mallick, and T. Sadhu, J. Stat. Mech.: Theory Exp. (2015) P09007.
[16] P. L. Krapivsky, K. Mallick, and T. Sadhu, Phys. Rev. Lett. **113**, 078101 (2014).
[17] C. Hegde, S. Sabhapandit, and A. Dhar, Phys. Rev. Lett. **113**, 120601 (2014).
[18] A. Poncet, A. Grabsch, P. Illien, and O. Benichou, Phys. Rev. Lett. **127**, 220601 (2021).
[19] A. Grabsch, A. Poncet, P. Rizkallah, P. Illien, and O. Bénichou, Sci. Adv. **8**, eabm5043 (2021).
[20] M. J. A. M. Brummelhuis and H. J. Hilhorst, Physica A **156**, 575 (1989).
[21] M. J. A. M. Brummelhuis and H. J. Hilhorst, J. Stat. Phys. **53**, 249 (1988).
[22] O. Bénichou and G. Oshanin, Phys. Rev. E **66**, 031101 (2002).

[23] P. Illien, O. Bénichou, C. Mejía-Monasterio, G. Oshanin, and R. Voituriez, Phys. Rev. Lett. **111**, 038102 (2013).

[24] O. Bénichou, A. Bodrova, D. Chakraborty, P. Illien, A. Law, C. Mejía-Monasterio, G. Oshanin, and R. Voituriez, Phys. Rev. Lett. **111**, 260601 (2013).

[25] P. Illien, O. Bénichou, G. Oshanin, and R. Voituriez, Phys. Rev. Lett. **113**, 030603 (2014).

[26] S. Leitmann and T. Franosch, Phys. Rev. Lett. **118**, 018001 (2017).

[27] S. Leitmann and T. Franosch, Phys. Rev. Lett. **111**, 190603 (2013).

[28] T. Imamura, K. Mallick, and T. Sasamoto, Commun. Math. Phys. **384**, 1409 (2021).

[29] B. D. Hughes, *Random Walks and Random Environments: Random Walks* (Oxford University Press, Oxford, 1995), Vol. 1.

[30] M. Abramowitz and I. Stegun, *Handbook of Mathematical Functions: with Formulas, Graphs, and Mathematical Tables* (Dover Publications, Mineola, NY, 1965).

[31] R. Arratia, Ann. Probab. **11**, 362 (1983).

[32] D. Ben-avraham and S. Havlin, *Diffusion and Reactions in Fractals and Disordered Systems* (Cambridge University Press, Cambridge, 2005).

[33] O. Bénichou, P. Illien, G. Oshanin, A. Sarracino, and R. Voituriez, Phys. Rev. Lett. **115**, 220601 (2015).

[34] P. L. Krapivsky, K. Mallick, and T. Sadhu, J. Stat. Phys. **160**, 885 (2015).

[35] T. Sadhu and B. Derrida, J. Stat. Mech.: Theory Exp. (2015) P09008.

[36] A. Poncet, O. Benichou, and P. Illien, Phys. Rev. E **103**, L040103 (2021).

[37] W. Woess, *Random Walks on Infinite Graphs and Groups* (Cambridge University Press, Cambridge, 2000), p. 334.